Journal of Integrative Neuroscience

J. Integr. Neurosci. **2026**; 25(9): 52929
https://doi.org/10.31083/JIN52929

Original Research

Longitudinal Changes in Hippocampal-Default Mode Network Connectivity and Cognition During Electroacupuncture Intervention in Type 2 Diabetes-Associated Cognitive Decline: A Pilot Resting-State fMRI Study

Lin Yao[1], Meng-yuan Li[1], Yan-ze Liu[2], Jia-zhen Cao[3], Zheng Lian[4], Hong-nan Zhu[4], Hai-peng Huang[4], Zhen Zhong[4,*], Hong-feng Wang[4,*]

[1]Institute of Acupuncture and Massage, Northeast Asian Institute of Traditional Chinese Medicine, Changchun University of Chinese Medicine, 130117 Changchun, Jilin, China
[2]Acupuncture and Tuina Center, The Third Affiliated Clinical Hospital of Changchun University of Chinese Medicine, 130117 Changchun, Jilin, China
[3]College of nursing, Changchun University of Chinese Medicine, 130117 Changchun, Jilin, China
[4]College of Acupuncture and Massage, Changchun University of Chinese Medicine, 130117 Changchun, Jilin, China
*Correspondence: zhongzhen930605@126.com (Zhen Zhong); wanghf@ccucm.edu.cn (Hong-feng Wang)
Academic Editors: Bernadette A. Murphy and Bettina Platt
Submitted: 15 April 2026 Revised: 9 July 2026 Accepted: 22 July 2026 Published: 21 September 2026

Abstract

Background: Type 2 diabetes mellitus-associated cognitive dysfunction (T2DACD) is strongly linked to disruption of cognition-supporting brain networks. Electroacupuncture (EA) has increasingly been examined as a nonpharmacological intervention targeting cognitive impairment; however, the longitudinal neurobiological patterns accompanying EA in T2DACD have not been fully characterized. In this exploratory pilot study, we evaluated alterations in resting-state functional connectivity (RSFC) across hippocampal subregions and default mode network (DMN) nodes in individuals with T2DACD. **Methods:** For this exploratory, open-label, non-randomized, uncontrolled pilot investigation, we enrolled 20 individuals with T2DACD and 26 healthy controls (HCs). Longitudinal analyses included 15 participants who had usable post-treatment data. T2DACD was defined according to clinical type 2 diabetes mellitus criteria, and a Montreal Cognitive Assessment (MoCA) score <26. Patients underwent an 8-week Adjust Zang-fu and Arouse Spirit electroacupuncture (AZASE) intervention. Cognitive, emotional, metabolic, and seed-based resting-state functional magnetic resonance imaging (rs-fMRI) outcomes were evaluated. Clinical longitudinal analyses were carried out according to protocol, whereas imaging analyses were limited to participants with usable scans after treatment. **Results:** At baseline, individuals with T2DACD showed lower MoCA scores than HCs and had poorer executive and working-memory outcomes. Among the 15 participants with complete longitudinal neuroimaging data, MoCA scores increased from 23.27 ± 1.71 to 26.07 ± 1.53 over the intervention period. Within-group alterations were observed for Flanker-conflict reaction time and accuracy, Stroop-conflict reaction time, 1-back reaction time, Self-Rating Anxiety Scale score, and Hamilton Depression Rating Scale score. Omnibus group analyses detected significant effects for the left anterior hippocampus-left angular gyrus connection and the left posterior hippocampus-right middle occipital gyrus connection. Post-treatment scans demonstrated reduced RSFC in several hippocampal-DMN and intra-DMN connections. The association between change in left anterior hippocampus-left angular gyrus RSFC and change in Stroop-conflict performance was no longer statistically significant after Bonferroni correction. For neuroimaging outcomes, cluster-level family-wise error (FWE) correction ($p < 0.05$) was applied to control for multiple comparisons; clinical outcomes are reported descriptively as hypothesis-generating findings. **Conclusions:** In this exploratory pilot study, we identified preliminary alterations in cognitive outcomes and hippocampal-DMN connections over an 8-week EA intervention in individuals with T2DACD. In view of the small sample size and the open-label, non-randomized, uncontrolled design, the findings should be interpreted as hypothesis-generating observations rather than definitive evidence of a specific causal treatment effect. Larger controlled studies will be needed to determine whether the observed neural and behavioral alterations are reproducible and clinically meaningful in practice. **Clinical Trial Registration:** No: ChiCTR2000040268, https://www.chictr.org.cn/hvshowproject.html?id=76145&v=1.3.

Keywords: electroacupuncture; diabetes mellitus, type 2; cognitive dysfunction; magnetic resonance imaging; hippocampus; default mode network

1. Introduction

Diabetes mellitus continues to be a major public health challenge worldwide. The International Diabetes Federation (IDF), type 2 diabetes mellitus (T2DM) affects hundreds of millions of adults worldwide and continues to impose a growing burden on healthcare systems [1,2]. Beyond its well-recognized metabolic and vascular complications, T2DM is widely recognized as a contributor to cognitive impairment, ranging from subtle diabetes-associated cognitive dysfunction to mild cognitive impairment and dementia [3]. Meta-analytic evidence indicates that adults with T2DM show mild-to-moderate deficits across several cognitive domains, particularly executive function, processing speed, attention, and memory [4]. Mild cognitive impairment also appears fairly common in this population, and the coexistence of diabetes and cognitive impairment may further increase the risk of progression to dementia [5,6]. These findings underscore the need to identify early neurocognitive changes in T2DM and to define mechanisms that may be modifiable.

Type 2 diabetes mellitus-associated cognitive dysfunction (T2DACD) refers to an early stage of cognitive deterioration in individuals with T2DM. It is typically manifested by reduced memory, attention, information-processing speed, and executive performance, without necessarily satisfying diagnostic criteria for dementia [3,4,7]. The pathophysiology of T2DACD is probably multifactorial and may involve chronic hyperglycemia, insulin resistance, microvascular injury, neuroinflammation, and disturbance of large-scale functional brain networks [7]. Even so, the association between T2DM and cognitive impairment remains underrecognized by patients and clinicians, which may delay detection and weaken timely management [3]. Current clinical management still focuses primarily on glycemic control and vascular risk reduction. Targeted strategies for diabetes-related cognitive dysfunction are still limited, and whether glucose lowering alone can prevent or reverse cognitive impairment is still uncertain [3,7]. Adjunctive nonpharmacological interventions with potential metabolic and neurocognitive benefits therefore merit further investigation.

Acupuncture, particularly electroacupuncture (EA), is increasingly being examined as a nonpharmacological therapeutic approach and peripheral neuromodulatory strategy for cognitive disorders. Clinical and experimental evidence suggest that acupuncture or EA may enhance cognitive outcomes in amnestic mild cognitive impairment, Alzheimer's disease, and post-stroke cognitive impairment [8,9,10]. In our previous studies on diabetes and related complications, a standardized EA protocol was linked to improved glucose regulation, attenuated insulin resistance, and reduced neuronal injury-related signaling in diabetic models [11,12]. Our previous resting-state functional magnetic resonance imaging (rs-fMRI) investigation also revealed abnormal functional connectivity between hippocampal subregions and the default mode network (DMN) in individuals with T2DACD [13]. Because the hippocampus and DMN are critical for memory processing and higher-order cognition, disruption of these networks may serve as an important neurobiological basis of diabetes-related cognitive dysfunction [14,15].

The hippocampus and the DMN each comprise functionally distinct subregions. Along the hippocampal long axis, the anterior portion is more strongly linked to emotional processing and memory encoding, whereas the posterior portion is more strongly engaged in spatial and contextual memory [16]. Within the DMN, the posterior cingulate/precuneus hub (DefaultC), the angular gyrus/lateral temporal hub (DefaultD), and the medial temporal hub (DefaultF) serve distinct yet complementary roles in self-referential processing, semantic cognition, and episodic memory, respectively [17,18]. Because T2DACD may affect both affective and cognitive domains, separate analysis of these specialized subregions may yield more precise insight than whole-network approaches. We therefore selected bilateral anterior, middle, and posterior hippocampal subregions, along with DefaultC, DefaultD, and DefaultF DMN subregions, as seeds for resting-state functional connectivity (RSFC) analyses.

On this basis, we carried out a prospective, open-label, uncontrolled pilot neuroimaging investigation to describe longitudinal alterations in cognition, emotional symptoms, metabolic measures, and hippocampal-centered RSFC during an 8-week standardized EA intervention in individuals with T2DACD. Because the investigation did not include a sham-acupuncture group or an attention-control T2DACD group, it was not intended to establish treatment efficacy or a causal mechanism. Instead, the aim was to detect preliminary clinical and neural signals and to develop hypotheses for future controlled trials [19,20,21].

2. Materials and Methods

2.1 Study Design and Participant Enrollment

This was a prospective, open-label, non-randomized, exploratory pilot intervention study. A non-diabetic healthy control group was included for baseline comparisons alone and did not serve as a longitudinal control.

We enrolled 26 healthy controls (HCs) and 20 participants with T2DACD. The two groups were matched as closely as feasible for age, sex, years of education, and handedness. HCs completed baseline clinical and rs-fMRI assessments only. Participants with T2DACD completed the same baseline assessments, received the Adjust Zang-fu and Arouse Spirit electroacupuncture (AZASE) intervention, and underwent post-treatment assessment.

The investigation was designed as an exploratory neuroimaging intervention investigation. Accordingly, the sample size was set pragmatically according to recruitment feasibility, participant burden, and magnetic resonance imaging (MRI) resource constraints.

Previous fMRI power analyses have shown that sample-size requirements depend on the study design, effect size, and statistical threshold, with samples of approximately 12–20 participants achieving about 80% power under specific experimental assumptions [22]. The final sample of 15 completers was within this range and provided initial estimates for planning future trials. Consistent with reporting recommendations for pilot and feasibility-oriented clinical studies, treatment effects should be interpreted in light of the exploratory nature of the investigation.

2.2 Eligibility Criteria for the T2DACD Group

Participants were eligible for the T2DACD group if they met the following criteria: (i) fulfilled the diagnostic criteria for T2DM according to the American Diabetes Association (ADA) Standards of Medical Care in Diabetes—2020 [23] and had a disease duration of at least 2 years; (ii) had evidence of cognitive dysfunction on standardized assessment, defined as a Montreal Cognitive Assessment (MoCA) score <26 [24]; (iii) were 50–70 years old, had underwent at least 6 years of education, and could complete the neuropsychological assessments; and (iv) were right-handed.

Participants were excluded if they had one or more of the following: (i) severe auditory, visual, or speech impairments; (ii) acute diabetic complications during the preceding 3 months; (iii) a history of clinically significant cerebrovascular disease, including cerebral infarction, intracerebral hemorrhage, vascular dementia, or other focal brain injury; (iv) alcohol or other substance abuse or dependence during the preceding 2 years; (v) other neurological or psychiatric disorders during the preceding 2 years; or (vi) MRI contraindications, such as claustrophobia or pacemaker implantation.

2.3 Eligibility Criteria for the Healthy Control Group

HCs were eligible if they were right-handed, were 50–70 years old, had underwent more than 6 years of education, and could complete the cognitive assessments.

Healthy controls were excluded if they had signs of cognitive impairment, severe cardiac, pulmonary, renal, neurological, or psychiatric disease, MRI contraindications, severe cranial deformity, or intracranial lesions.

2.4 Study Procedure and Outcome Assessments

HCs underwent clinical evaluation and rs-fMRI scanning at baseline only (time point 1, TP1). Participants with T2DACD completed the same baseline assessments at TP1 and were reevaluated after completing the AZASE intervention (time point 2, TP2).

Laboratory assessments included glucose and lipid metabolism indices, including fasting plasma glucose (FPG), hemoglobin A1c (HbA1c), total cholesterol (TC), triglycerides (TG), high-density lipoprotein cholesterol (HDL-C), and low-density lipoprotein cholesterol (LDL-C). Cognitive assessment comprised the MoCA as a global cognitive screening measure, along with task-based tests for specific cognitive domains: the Flanker task to assess attentional inhibition, the Stroop task to assess conflict pro-

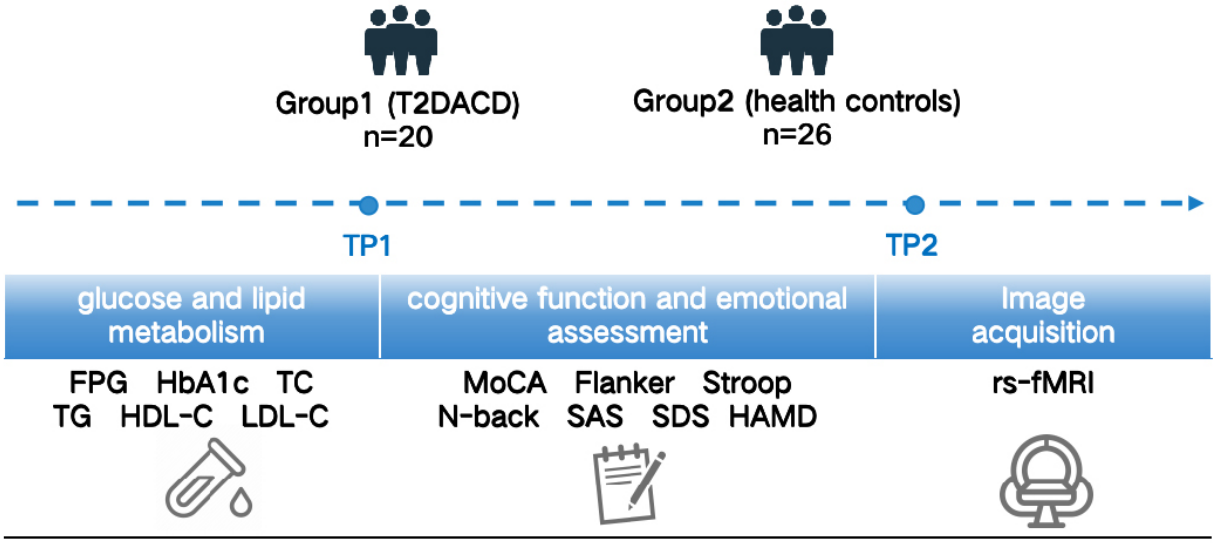

Fig. 1. Study overview. Abbreviations: HCs, healthy controls; T2DACD, Type 2 diabetes mellitus-associated cognitive dysfunction; TP1, time point 1; TP2, time point 2; FPG, fasting plasma glucose; HbA1c, hemoglobin A1c; TC, total cholesterol; TG, triglycerides; HDL-C, high-density lipoprotein cholesterol; LDL-C, low-density lipoprotein cholesterol; MoCA, Montreal Cognitive Assessment; SAS, Self-Rating Anxiety Scale; SDS, Self-Rating Depression Scale; HAMD, Hamilton Depression Rating Scale; rs-fMRI, resting-state functional magnetic resonance imaging.

cessing, and the N-back task to assess working memory. Affective status was evaluated using the Self-Rating Anxiety Scale (SAS), Self-Rating Depression Scale (SDS), and Hamilton Depression Rating Scale (HAMD).

The HC group was included to provide a non-diabetic baseline reference for demographic, cognitive, and neuroimaging comparisons, and not as a longitudinal treatment-control group (Fig. 1).

2.5 "Adjust Zang-fu and Arouse Spirit" Electroacupuncture (AZASE) Treatment

Patients in the T2DACD group underwent the AZASE intervention. All treatment sessions were administered by licensed acupuncturists in China, each having at least 3 years of clinical acupuncture experience. Acupoints were identified according to the National Standard of the People's Republic of China, Nomenclature and location of acupuncture points (GB/T 12346-2006) [25].

The chosen acupoints were GV20 (Baihui), GV24 (Shenting), bilateral BL13 (Feishu), BL20 (Pishu), BL23 (Shenshu), LI4 (Hegu), LR3 (Taichong), ST36 (Zusanli), and SP6 (Sanyinjiao) (Fig. 2). With each participant in a comfortable seated position, sterile filiform needles (0.3 mm × 25 mm or 0.3 mm × 40 mm; Hwato, Suzhou Medical Appliance Factory, Suzhou, Jiangsu, China) were inserted into the selected acupoints. Needling depth varied according to the anatomical site: GV24 and GV20 were needled subcutaneously at a 15° angle to depths of 10–20 mm and 20–30 mm, respectively; BL13 and BL20 were needled obliquely toward the spine at a 30–45° angle to a depth of 20–30 mm; BL23 was needled perpendicularly to a depth of 20–35 mm; ST36 and SP6 were needled perpendicularly to a depth of 30–40 mm; and LI4 and LR3 were needled perpendicularly to a depth of 20–30 mm. Manual manipulation was then applied to elicit deqi sensation. Thereafter, an SDZ-V electroacupuncture device (Suzhou Medical Appliance Factory, Suzhou, China) was connected to GV20-GV24, unilateral BL20-BL23, and bilateral SP6-LR3. Electrical stimulation was provided using a alternating 2/100-Hz stimulation and 0.1–1.0 mA for approximately 30 minutes per session, once per day, 5 days per week, over 8 consecutive weeks.

2.6 rs-fMRI Scanning Parameters

Magnetic resonance imaging (MRI) data were obtained with a Siemens 3.0-T scanner (3T MAGNETOM Trio; software version VB17A; Siemens AG, Henkestrasse 127, Erlangen, Bavaria, Germany; Department of Radiology, Affiliated Hospital of Changchun University of Chinese Medicine). Foam padding was placed around each participant's head to limit motion during image acquisition. During rs-fMRI, participants were asked to keep their eyes closed, remain awake, relax without falling asleep, and avoid intentional mental activity.

High-resolution three-dimensional T1-weighted anatomical images were acquired with the following parameters: repetition time (TR) = 2300 ms; echo time (TE) = 3.33 ms; field of view (FOV) = 256 × 256 mm; voxel size = 1.0 × 1.0 × 1.0 mm; and slice thickness = 1 mm. Resting-state blood-oxygen-level-dependent (BOLD) images were collected using single-shot gradient-recalled echo-planar imaging (EPI) with TR = 3000 ms, TE = 30 ms, FOV = 220 × 220 mm, voxel size = 3.4 × 3.4 × 3.0 mm, and slice thickness = 3 mm. Each EPI run comprised 128 time points (volumes). At least two EPI runs were completed by each participant to improve the stability of the BOLD signal and to reduce the influence of run-specific variability.

2.7 MRI Preprocessing

Preprocessing of the MRI data was performed using MRIcroGL (version 1.2.20220720; University of South Carolina, Columbia, SC, USA), FSL (version 6.0.6.2; Oxford Centre for Functional MRI of the Brain, Oxford, UK), and SPM12 (r7771; Wellcome Centre for Human Neuroimaging, London, UK), all implemented in MATLAB (R2025b; The MathWorks, Inc., Natick, MA, USA). The preprocessing pipeline consisted of: (1) conversion from Digital Imaging and Communications in Medicine (DICOM) to Neuroimaging Informatics Technology Initiative (NIfTI) format; (2) removal of the first four volumes to allow magnetization to reach equilibrium; (3) slice-timing correction; (4) realignment to correct for head motion; (5) co-registration of functional images to the structural image; (6) normalization to Montreal Neurological Institute (MNI)-152 space and resampling to 3 × 3 × 3 mm^3; (7) spatial smoothing with a 6-mm full-width at half-maximum Gaussian kernel; and (8) temporal band-pass filtering between 0.01 and 0.08 Hz, followed by linear detrending.

Participants were excluded from neuroimaging analyses when head motion exceeded 1 mm in translation or 1° in rotation in any direction during preprocessing. This quality-control criterion was specified before analysis and was applied uniformly across participants. Framewise displacement (FD) was calculated as an additional index of volume-to-volume motion. FD values were computed for each participant as the sum of absolute changes in the six motion parameters. Volume censoring (scrubbing) was not applied. Nuisance regression included signals from white matter and cerebrospinal fluid, but global signal regression was not used. Motion parameters were not included in the nuisance regression model. Because denoising strategies can materially influence RSFC estimates, these preprocessing decisions are reported in detail [26,27].

Seed-based RSFC analyses were carried out with predefined regions of interest (ROI). Hippocampal subregions were separated along the longitudinal axis into anterior, middle, and posterior portions following the segmentation approach established in Xie et al. [16]. DMN subregions

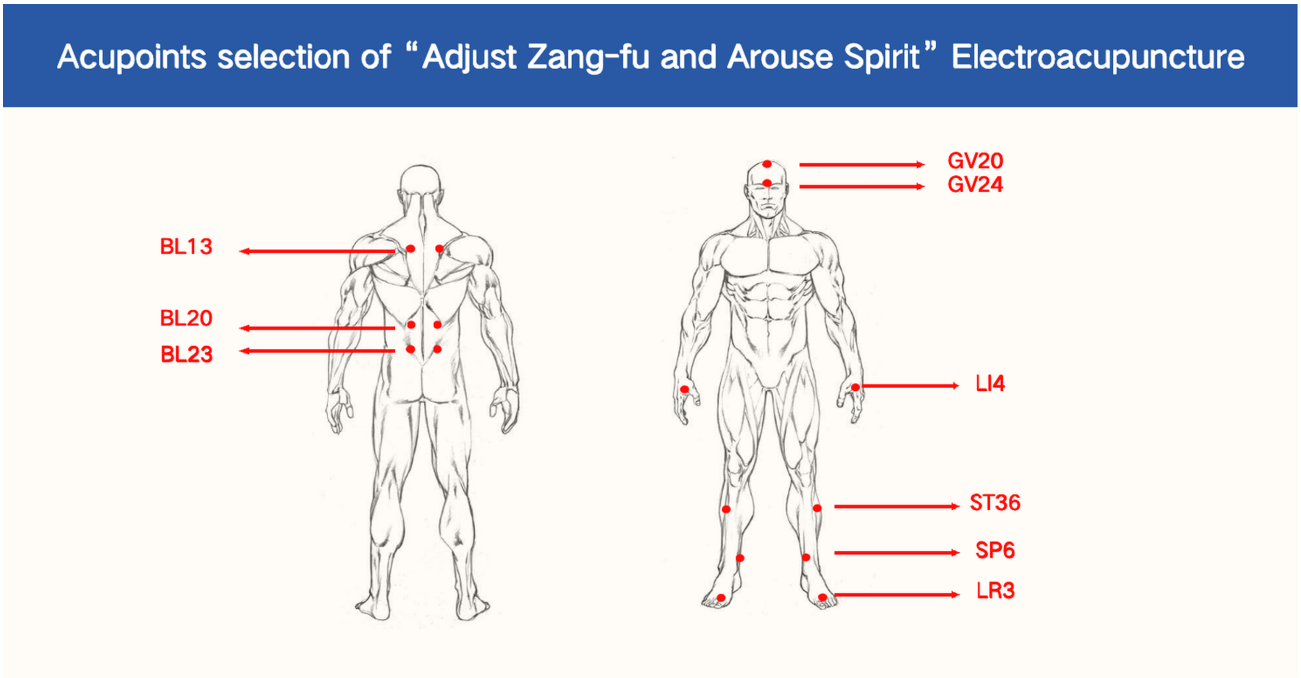

Fig. 2. Acupoint location diagram for "Adjust Zang-fu and Arouse Spirit" electroacupuncture. GV20, Baihui; GV24, Shenting; BL13, Feishu; BL20, Pishu; BL23, Shenshu; LI4, Hegu; LR3, Taichong; ST36, Zusanli; SP6, Sanyinjiao.

(DefaultC, DefaultD, and DefaultF) were defined using seed coordinates derived from the Yeo 7-network parcellation study [17]. The functional characterization of these DMN subregions follows the three-subsystem model proposed by Andrews-Hanna et al. [28]. ROI masks were constructed in MNI space and were visually checked after registration to each participant's normalized functional image. For each ROI, the mean time series was extracted and correlated with every other brain voxel; the resulting correlation coefficients were then converted to z values through Fisher's r-to-z transformation.

2.8 Statistical Assessment

This work was designed as an exploratory pilot investigation, not as a confirmatory trial powered for formal hypothesis testing. Nevertheless, several outcomes were prespecified to provide a structured descriptive assessment. The primary clinical measure was the Montreal Cognitive Assessment (MoCA) score, which served as a measure of overall cognitive performance. The primary neuroimaging outcome was the longitudinal alteration in hippocampal-DMN RSFC. Additional and exploratory endpoints incorporated task-related cognitive performance on the Flanker, Stroop, and N-back tasks; affective outcomes, involving SAS, SDS, and HAMD values; and metabolism-related indicators, including FPG, HbA1c, TC, TG, HDL-C, and LDL-C. These variables were analyzed descriptively to support hypothesis generation for subsequent well-controlled investigations, and the findings should be viewed in that context.

2.8.1 Clinical Dataset Evaluation

Clinical data were analyzed using IBM SPSS Statistics 26 (IBM, Armonk, NY, USA). Continuous variables are reported as means with standard deviations (SDs), and categorical variables are reported as counts with percentages. Initial differences between HCs and participants with T2DACD were assessed with independent-samples *t*-tests or chi-square tests, as appropriate for the data type. For longitudinal analyses, the distribution of each shift score (TP2-TP1) was checked with the Shapiro-Wilk test and by visual inspection of Q-Q plots. Variables satisfying the normality assumption (Shapiro-Wilk $p > 0.05$) were analyzed with paired-samples *t*-tests, whereas variables that violated this assumption were analyzed with the non-parametric Wilcoxon signed-rank test. All statistical tests were two-sided. Because the study was exploratory and involved multiple measures, the findings were interpreted carefully.

Given the exploratory nature of the present work, no adjustment for multiplicity was used to *p* values for the cognitive, affective, or metabolic measures. The pilot work was intended to estimate initial effect sizes and assess feasibility rather than to provide definitive data [20]. Accordingly, effect sizes and 95% confidence intervals are reported together with *p* values throughout the Results section [29]. These results should be interpreted descriptively, and all variables are presented for completeness and transparency regardless of statistical significance.

Sensitivity statistical analysis with linear mixed-effects statistical models. To test whether the paired-samples *t*-test findings were stable to individual-level vari-

ability, we conducted sensitivity evaluations using linear mixed-effects models (LMMs) for all longitudinal continuous measures. Each LMM comprised time point (TP1 versus TP2) as a fixed association and individual as a random intercept, with age and sex entered as covariates. Restricted maximum likelihood (REML) estimation was applied, and degrees of freedom were approximated using the Satterthwaite method.

2.8.2 Functional Coupling Assessment

Seed-based functional coupling statistical analyses were performed in SPM12 with predefined hippocampal and DMN subregions used as ROI. Bilateral anterior, middle, and posterior hippocampal subregions, together with the DefaultC, DefaultD, and DefaultF DMN subregions, were specified as seed areas. For each seed, the mean time series was extracted and correlated with the time series of all other brain voxels to generate whole-brain functional connectivity (FC) maps. These maps were then converted into z-score maps with Fisher's r-to-z transformation.

For group-level imaging analyses, statistical procedures were selected according to the structure of the dataset. Exploratory omnibus comparisons were initially conducted using one-way ANOVA to examine overall differences among HCs, T2DACD patients before intervention (TP1), and T2DACD patients after intervention (TP2). However, because TP1 and TP2 measurements were obtained from the same participants, these observations were not statistically independent. Therefore, ANOVA findings were interpreted only as exploratory omnibus results rather than definitive between-group comparisons. Formal longitudinal effects within the T2DACD cohort were assessed using paired-samples *t*-tests comparing TP1 and TP2 measurements. Baseline differences between HCs and T2DACD participants were evaluated using appropriate independent-group comparisons. Age and sex were incorporated as covariates in the imaging models. Education was regarded as a potential confounder but was not comprised in the main statistical model given that years of education did not differ significantly between cohorts at initial. Dia-

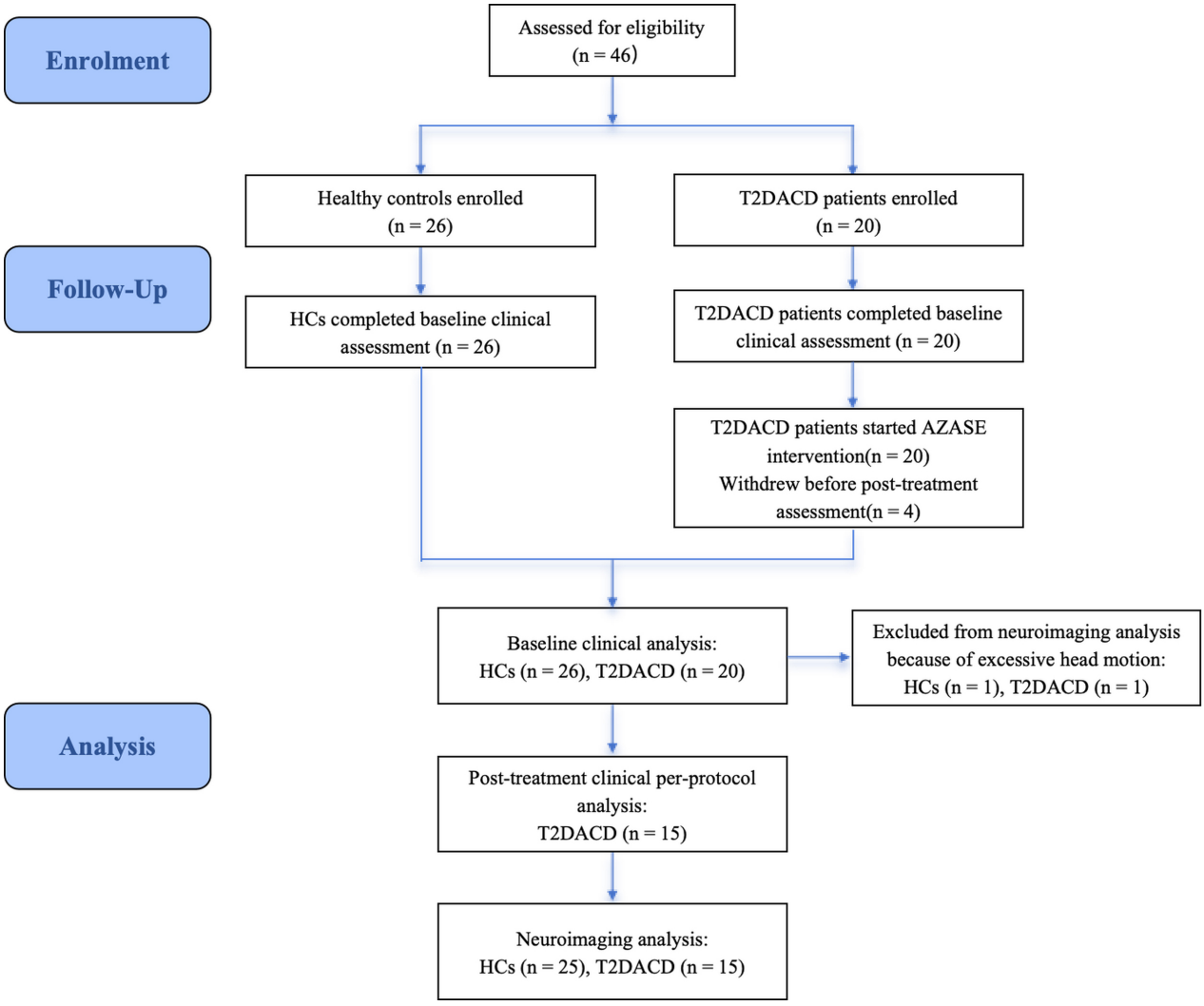

Fig. 3. Participant flow diagram. AZASE, Adjust Zang-fu and Arouse Spirit electroacupuncture.

betes duration was additionally clinically relevant; nevertheless, it was available only for the T2DACD group and thus could not be modeled consistently in analyses that comprised HCs. Residual confounding related to education or diabetes-related clinical variability thus could not be completely excluded.

The HC cohort was used only as a non-diabetic initial comparison for describing disease-related abnormalities at TP1. The cross-sectional contrast between T2DACD-TP2 and HCs was conducted for descriptive visualization solely, mainly to examine whether postintervention coupling values indicated a directional trend toward the HC comparison profile. The present descriptive comparison was not intended to test intervention effectiveness, and no inferential claim was made that the TP2 coupling pattern had normalized relative to HCs.

Multiple contrasts in the imaging evaluations were controlled with cluster-based inference based on random field theory [30]. The voxel-level cluster-forming cutoff was set at $p < 0.005$ (uncorrected), and clusters were regarded statistically significant if they survived cluster-level family-wise error (FWE) adjustment at $p < 0.05$. This threshold-based strategy is commonly applied in fMRI research and has been described as offering a practical balance between Type I and Type II error, particularly in exploratory investigations with restricted small sample sizes [31]. The cluster-extent cutoff (k) was derived from the estimated smoothness of the dataset and corresponded to a corrected cluster-level $p < 0.05$. Although a voxel-level threshold of $p < 0.005$ is less conservative than $p < 0.001$, it increases sensitivity for detecting limited but potentially meaningful associations, which is frequently notable in hypothesis-generating pilot neuroimaging studies [31]. We nevertheless acknowledge that this approach might increase the risk of false-positive observations. Therefore, all imaging findings should be regarded as initial and should be confirmed in independent samples using greater stringent correction procedures [32].

2.8.3 Correlation Evaluation

To examine whether treatment-related neural alterations were related to clinical change, partial correlation evaluations were performed within the T2DACD cohort. Shifts in RSFC (ΔRSFC, TP2 - TP1) were correlated with alterations in clinical measures (Δclinical outcomes, TP2 - TP1), with age and sex included as covariates. Bonferroni adjustment was used across the designed correlation tests. After adjustment, statistical significance was defined using the Bonferroni-adjusted alpha level.

3. Results

3.1 Individual Flow and Initial Characteristics

A total of 46 individuals were enrolled, comprising 26 HCs and 20 participants with T2DACD. All individuals completed the initial clinical assessment. During follow-up, four individuals in the T2DACD cohort voluntarily withdrew before completing the 8-week treatment. In addition, one HC and one individual with T2DACD were excluded from the neuroimaging evaluation given that head motion exceeded the prespecified quality-control cutoff of 1 mm translation or 1° rotation during preprocessing. Consequently, initial clinical contrasts included 26 HCs and 20 participants with T2DACD, whereas longitudinal postintervention clinical and neuroimaging evaluations were based on the 15 T2DACD individuals who completed the treatment and had usable postintervention datasets (Fig. 3). The HC cohort served as an initial comparison group rather than as a longitudinal comparator.

Initial demographic and metabolism-related characteristics at TP1 are reported in Table 1, and initial cognitive and affective indices at TP1 are reported in Table 2. No statistically significant between-group differences were observed in age, sex distribution, years of education, height, weight, TC, TG, HDL-C, or LDL-C (all $p > 0.05$). As expected, the T2DACD cohort had significantly higher FPG and HbA1c levels than the HC cohort (both $p < 0.001$).

Compared with HCs, participants with T2DACD had lower MoCA values and poorer task performance on several task-related outcomes. Specifically, the T2DACD cohort demonstrated lower accuracy in the Flanker no-conflict, Stroop consistency, Stroop-conflict, and 1-back conditions, as well as longer response times in the Flanker no-conflict, Flanker interference, Stroop neutrality, Stroop consistency, Stroop-conflict, 1-back, and 2-back conditions (all $p < 0.05$). No statistically significant between-group differences were detected for SAS, SDS, or HAMD values.

To evaluate possible attrition bias, initial characteristics were compared between completers (n = 15) and non-completers (n = 5) in the T2DACD cohort with Welch's *t*-tests and Fisher's exact test (**Supplementary Table 1**). The two subgroups were comparable in age, sex, education, diabetes duration, MoCA score, Hachinski Ischemic Score, glycemic markers (FPG and HbA1c), and all task-related cognitive outcomes (Flanker, Stroop, and N-back tasks; all $p > 0.10$). Completers had numerically higher baseline SAS ($p = 0.030$), HAMD ($p = 0.001$), and TC ($p = 0.012$) scores and lower HDL-C ($p = 0.034$) than non-completers; however, these contrasts involved solely five non-completers and should be read descriptively. Importantly, the absence of initial differences in the primary cognitive and metabolism-related measures suggests that the completer subsample was reasonably representative of the enrolled T2DACD group for the primary work measures.

3.2 Clinical Alterations in the T2DACD Cohort After AZASE

All longitudinal contrasts presented below were also examined using linear mixed-effects statistical models with individual entered as a random intercept and age and sex entered as fixed covariates. These sensitivity analyses led

Table 1. Demographic and metabolic characteristics at TP1.

Variable	HCs (n = 26)	T2DACD (n = 20)	*p* value (HC vs T2DACD at TP1)
Age, years	55.69 (5.55)	58.70 (4.88)	0.061
Male, n (%)	7 (26.9)	10 (50.0)	0.108
Female, n (%)	19 (73.1)	10 (50.0)	—
Education, years	11.46 (2.47)	11.85 (2.41)	0.596
Duration of diabetes, years	—	9.8 (6.68)	—
Height, m	1.63 (0.05)	1.67 (0.08)	0.052
Weight, kg	63.17 (6.71)	67.65 (8.63)	0.054
FPG, mmol/L	5.52 (0.24)	8.71 (3.27)	<0.001
HbA1c, %	5.58 (0.18)	7.54 (1.68)	<0.001
TC, mmol/L	4.87 (1.11)	5.05 (0.78)	0.561
TG, mmol/L	2.02 (1.46)	2.15 (1.31)	0.750
HDL-C, mmol/L	1.32 (0.22)	1.20 (0.21)	0.065
LDL-C, mmol/L	3.25 (0.90)	3.45 (0.87)	0.465

Data are presented as mean (SD) unless otherwise indicated.

Table 2. Cognitive and emotional assessments at TP1.

Variable	HCs (n = 26)	T2DACD (n = 20)	*p* value (HCs vs T2DACD at TP1)
MoCA score	27.35 (1.16)	23.20 (1.74)	<0.001
Flanker-no conflict			
reaction time, s	0.54 (0.08)	0.70 (0.17)	<0.001
accuracy rate	0.99 (0.02)	0.92 (0.07)	<0.001
Flanker-conflict			
reaction time, s	0.60 (0.07)	0.74 (0.18)	0.003
accuracy rate	0.93 (0.06)	0.90 (0.06)	0.077
Stroop-neutrality			
reaction time, s	0.77 (0.16)	0.99 (0.26)	0.002
accuracy rate	0.98 (0.06)	0.93 (0.09)	0.053
Stroop-consistency			
reaction time, s	0.76 (0.16)	0.99 (0.26)	0.002
accuracy rate	0.98 (0.06)	0.93 (0.09)	0.04
Stroop-conflict			
reaction time, s	0.88 (0.13)	1.11 (0.27)	0.002
accuracy rate	0.94 (0.07)	0.82 (0.17)	0.005
1-back			
reaction time, s	0.68 (0.13)	1.02 (0.23)	<0.001
accuracy rate	0.90 (0.08)	0.83 (0.08)	0.007
2-back			
reaction time, s	0.95 (0.29)	1.33 (0.41)	0.001
accuracy rate	0.74 (0.07)	0.75 (0.08)	0.811
SAS score	27.54 (2.94)	29.65 (4.22)	0.065
SDS score	27.04 (0.47)	28.30 (4.45)	0.224
HAMD score	4.00 (1.39)	3.80 (2.28)	0.614

Data are presented as mean (SD).

to conclusions aligned with the paired-samples analyses (**Supplementary Table 2**). The direction, magnitude, and statistical significance of the LMM-derived time within-group effects were aligned with the paired *t*-test findings (see **Supplementary Table 2**). For ease of interpretation, paired *t*-test findings are therefore presented as the main analyses, with LMM findings reported as definitive sensitivity evaluations.

Table 3 summarizes metabolism-related characteristics and affective markers before and after intervention (TP1 and TP2). During the 8-week treatment period, the T2DACD cohort indicated multiple within-group shifts in

Table 3. Longitudinal metabolic and emotional outcomes in the T2DACD group.

Variable	T2DACD-TP1 (n = 15)	T2DACD-TP2 (n = 15)	Mean change (TP2-TP1)	95% CI of change	dz	*p* value (TP1 vs TP2)
FPG, mmol/L	8.58 (3.65)	7.29 (1.28)	–1.29	–2.85 to 0.27	0.40	0.102
HbA1c, %	7.49 (1.73)	7.15 (1.06)	–0.34	–0.76 to 0.08	0.44	0.116
TC, mmol/L	5.24 (0.78)	5.01 (0.68)	–0.23	–0.74 to 0.28	0.23	0.367
TG, mmol/L	2.17 (1.49)	1.85 (0.86)	–0.32	–1.14 to 0.50	0.21	0.443
HDL-C, mmol/L	1.14 (0.18)	1.12 (0.19)	–0.02	–0.11 to 0.07	0.11	0.673
LDL-C, mmol/L	3.57 (0.96)	3.60 (0.54)	0.03	–0.51 to 0.57	0.03	0.913
SAS score	30.47 (4.53)	28.20 (2.31)	–2.27	–3.75 to –0.78	0.85	0.006
SDS score	28.47 (4.93)	27.33 (2.87)	–1.14	–2.44 to 0.16	0.48	0.084
HAMD score	4.20 (1.45)	3.73 (0.70)	–0.47	–0.82 to –0.11	0.73	0.014

Data are presented as mean (SD).

Note: Positive mean change indicates increase from TP1 to TP2; negative mean change indicates decrease. Effect sizes (Cohen's dz) are reported for within-group changes. *p* values are uncorrected for multiple comparisons; given the exploratory nature of this pilot study, these should be interpreted descriptively. For variables that violated the normality assumption (SDS and HAMD scores), *p* values are from Wilcoxon signed-rank tests; for all other variables, *p* values are from paired-samples *t*-tests. Emphasis should be placed on effect sizes and confidence intervals rather than on *p* values alone.

cognitive and affective indices. MoCA scores showed a significant increase from 23.27 ± 1.71 at TP1 to 26.07 ± 1.53 at TP2 ($p < 0.001$). Statistically significant pre-to-post differences were also observed in Flanker-conflict response time, Flanker-conflict accuracy, Stroop-conflict response time, and 1-back reaction time. In addition, SAS and HAMD values showed decreased significantly during the treatment period, whereas FPG and HbA1c indicated non-significant downward trends.

Given that repeated assessments were performed solely in the T2DACD cohort, these longitudinal alterations should be viewed with caution. Repeated administration of the MoCA and computerized executive-control/working memory tasks may be affected by retest associations, and the absence of a repeatedly evaluated T2DACD appropriate control cohort prevents separation of intervention-associated change from retest-related alteration.

Normality of the shift values was evaluated using the Shapiro-Wilk test, as described in the Methods section. Variables that violated the normality assumption (SDS and HAMD values) were evaluated with non-parametric methods, specifically the Wilcoxon signed-rank test, as indicated in the table notes.

Table 4 summarizes cognitive indicators before and after intervention (TP1 and TP2). All variables, regardless of statistical significance, are reported with mean shifts, 95% confidence intervals, effect sizes (Cohen's dz), and *p* values. Approximate large within-group associations were observed for Flanker-conflict response time (mean alteration, –0.08 s; 95% CI, –0.14 to –0.03; dz ≈ –0.80), Flanker-conflict accuracy (mean alteration, 0.05; 95% CI, 0.01 to 0.08; dz ≈ 0.81), Stroop-conflict response time (mean shift, −0.09 s; 95% CI, –0.22 to –0.04; dz ≈ −0.37), 1-back response time (mean alteration, –0.17 s; 95% CI, –0.30 to –0.03; dz ≈ –0.66). These effect-size estimates should be regarded as preliminary because of the uncontrolled design and small sample size.

Overall, the clinical dataset suggest changes in overall cognitive function, specific executive-control and working memory outcomes, and certain affective symptoms over the treatment period. However, the current design does not allow firm attribution of these alterations to AZASE itself.

Given that the sample was small, effect sizes and confidence intervals are emphasized alongside *p* values, as these estimates are more informative than statistical significance tests alone in pilot investigations [33].

3.3 RSFC Alterations in the T2DACD Cohort Before and After Acupuncture Treatment

To assess alterations in brain functional network systems across the treatment period, RSFC was compared across initial HCs, pre-treatment T2DACD, and postintervention T2DACD. Significant omnibus group associations were detected for the left anterior hippocampus-left angular gyrus (aHPC.L-ANG.L) connection and the left posterior hippocampus-right middle occipital gyrus (pHPC.L-MOG.R) connection (Table 5, Fig. 4).

Within the T2DACD group, paired TP1-versus-TP2 contrasts indicated significantly decreased RSFC after AZASE in the following connections: left posterior hippocampus (pHPC.L)-right middle occipital gyrus (MOG.R), right middle temporal gyrus (MTG.R)-left precuneus (PCUN.L), left posterior cingulate gyrus (PCG.L)-left inferior frontal gyrus, orbital part (ORBinf.L), and right posterior cingulate gyrus (PCG.R)-left superior frontal gyrus, medial orbital part (ORBsupmed.L) (Table 5, Fig. 4). Visual inspection of the extracted mean z values from the statistically significant clusters suggested that, for multiple connections, the post-treatment T2DACD profile moved toward the HC reference pattern.

Table 4. Longitudinal cognitive outcomes in the T2DACD group.

Variable	T2DACD-TP1 (n = 15)	T2DACD-TP2 (n = 15)	Mean change (TP2-TP1)	95% CI of change	dz	*p* value (TP1 vs TP2)
MoCA score	23.27 (1.71)	26.07 (1.53)	2.80	2.04 to 3.56	2.04	<0.001
Flanker-no conflict						
reaction time, s	0.71 (0.17)	0.69 (0.19)	–0.02	–0.07 to 0.03	-0.24	0.368
accuracy rate	0.93 (0.07)	0.94 (0.04)	0.01	–0.01 to 0.03	0.27	0.359
Flanker-conflict						
reaction time, s	0.74 (0.17)	0.66 (0.14)	–0.08	–0.14 to –0.03	–0.80	0.008
accuracy rate	0.89 (0.06)	0.94 (0.06)	0.05	0.01 to 0.08	0.81	0.011
Stroop-neutrality						
reaction time, s	1.05 (0.32)	0.96 (0.23)	–0.09	–0.22 to 0.04	–0.37	0.175
accuracy rate	0.93 (0.14)	0.95 (0.07)	0.02	–0.07 to 0.11	0.10	0.711
Stroop-consistency						
reaction time, s	1.01 (0.25)	0.96 (0.29)	–0.05	–0.20 to 0.10	–0.17	0.526
accuracy rate	0.93 (0.10)	0.93 (0.09)	0.00	–0.06 to 0.06	–0.03	0.889
Stroop-conflict						
reaction time, s	1.11 (0.25)	0.98 (0.19)	–0.13	–0.22 to –0.04	–0.76	0.011
accuracy rate	0.84 (0.13)	0.87 (0.13)	0.03	–0.05 to 0.11	0.20	0.434
1-back						
reaction time, s	1.04 (0.23)	0.87 (0.30)	–0.17	–0.30 to –0.03	–0.66	0.023
accuracy rate	0.85 (0.08)	0.90 (0.07)	0.05	–0.00 to 0.10	0.53	0.055
2-back						
reaction time, s	1.33 (0.41)	1.25 (0.28)	–0.08	–0.22 to 0.06	–0.29	0.277
accuracy rate	0.75 (0.09)	0.76 (0.09)	0.01	–0.02 to 0.04	0.16	0.559

Data are presented as mean (SD).

Note: Positive mean change indicates an increase from TP1 to TP2; negative mean change indicates a decrease. Effect sizes (Cohen's dz) are reported for within-group changes. *p* values are uncorrected for multiple comparisons; given the exploratory nature of this pilot study, these should be interpreted descriptively. *p* values were obtained using paired-samples *t*-tests. Emphasis should be placed on effect sizes and confidence intervals rather than on *p* values alone.

3.4 Correlation Evaluation Findings

Exploratory correlation evaluations were conducted to examine whether treatment-related RSFC shifts were associated with shifts in clinical endpoints. The observed change in RSFC between the left anterior hippocampus and left angular gyrus was inversely correlated with alteration in Stroop-conflict response time (r = –0.608, uncorrected *p* = 0.027) (Fig. 5). Nevertheless, the present association did not remain statistically significant after Bonferroni adjustment.

No other significant associations were found between ΔRSFC and Δclinical measures. Therefore, the aHPC.L-ANG.L result should be viewed as a non-significant trend and as a hypothesis-generating observation only, rather than as data of a confirmed imaging-behavior pathway.

4. Discussion

4.1 Cognitive Clinical Outcomes

In this exploratory, open-label, uncontrolled pilot investigation, participants with T2DACD demonstrated poorer overall cognitive function and weaker task-related executive-control and working memory task performance than HCs at initial. This profile is generally aligned with previous data indicating that type 2 diabetes is associated with deficits in mnemonic, executive-control performance, processing speed, and attention, and that diabetes-related cognitive dysfunction ranges from subtle decline to mild cognitive impairment and dementia [3,4]. During the 8-week treatment period, the T2DACD group showed an increase in overall cognitive task performance, reflected by higher MoCA values, as well as pre-to-post shifts in selected outcomes of attentional appropriate control, interference processing, and working mnemonic. Anxiety and depressive symptom values decreased, whereas metabolism-related markers indicated only non-significant downward trends. Because these alterations occurred without a control group, they could not be attributed specifically to AZASE and might partly reflect retest associations, expectation-related, regression to the mean, or other non-specific influences. Given that the MoCA is widely applied as a screening measure for mild cognitive impairment, the postintervention increase may have possible clinical relevance, although the present careful interpretation must remain cautious [34].

Table 5. Group-level and within-group resting-state functional connectivity results.

Seed ROI	Target region	Comparison	Direction of effect	Cluster size (voxels)	Peak MNI x	Peak MNI y	Peak MNI z	Peak statistic
aHPC.L	ANG.L	HCs vs T2DACD-TP1 vs T2DACD-TP2	omnibus group effect	319	–52	–60	28	F = 13.9524
pHPC.L	MOG.R	HCs vs T2DACD-TP1 vs T2DACD-TP2	omnibus group effect	385	44	–76	4	F = 12.2973
pHPC.L	MOG.R	T2DACD-TP2 < T2DACD-TP1	decreased RSFC after treatment	385	44	–82	–6	T = –6.0831
MTG.R	PCUN.L	T2DACD-TP2 < T2DACD-TP1	decreased RSFC after treatment	292	–14	–70	36	T = –5.1200
PCG.L	ORBinf.L	T2DACD-TP2 < T2DACD-TP1	decreased RSFC after treatment	349	–44	36	–10	T = –4.7151
PCG.R	ORBsupmed.L	T2DACD-TP2 < T2DACD-TP1	decreased RSFC after treatment	336	10	42	–12	T = –4.6482

Note: Statistical significance was determined using a voxel-level cluster-defining threshold of $p < 0.005$ (uncorrected) and a cluster-level FWE-corrected threshold of $p < 0.05$, with a cluster-extent threshold (k) determined based on the estimated smoothness of the data. Peak F values are reported for omnibus group comparisons; peak T values are reported for paired pre-post comparisons within the T2DACD group. All reported clusters survived cluster-level FWE correction ($p < 0.05$).

Abbreviations: aHPC, anterior hippocampus; pHPC, posterior hippocampus; MOG, middle occipital gyrus; ANG, angular gyrus; MTG, middle temporal gyrus; PCUN, precuneus; PCG, posterior cingulate gyrus; ORBinf, inferior frontal gyrus, orbital part; ORBsupmed, superior frontal gyrus, medial orbital; FWE, family-wise error.

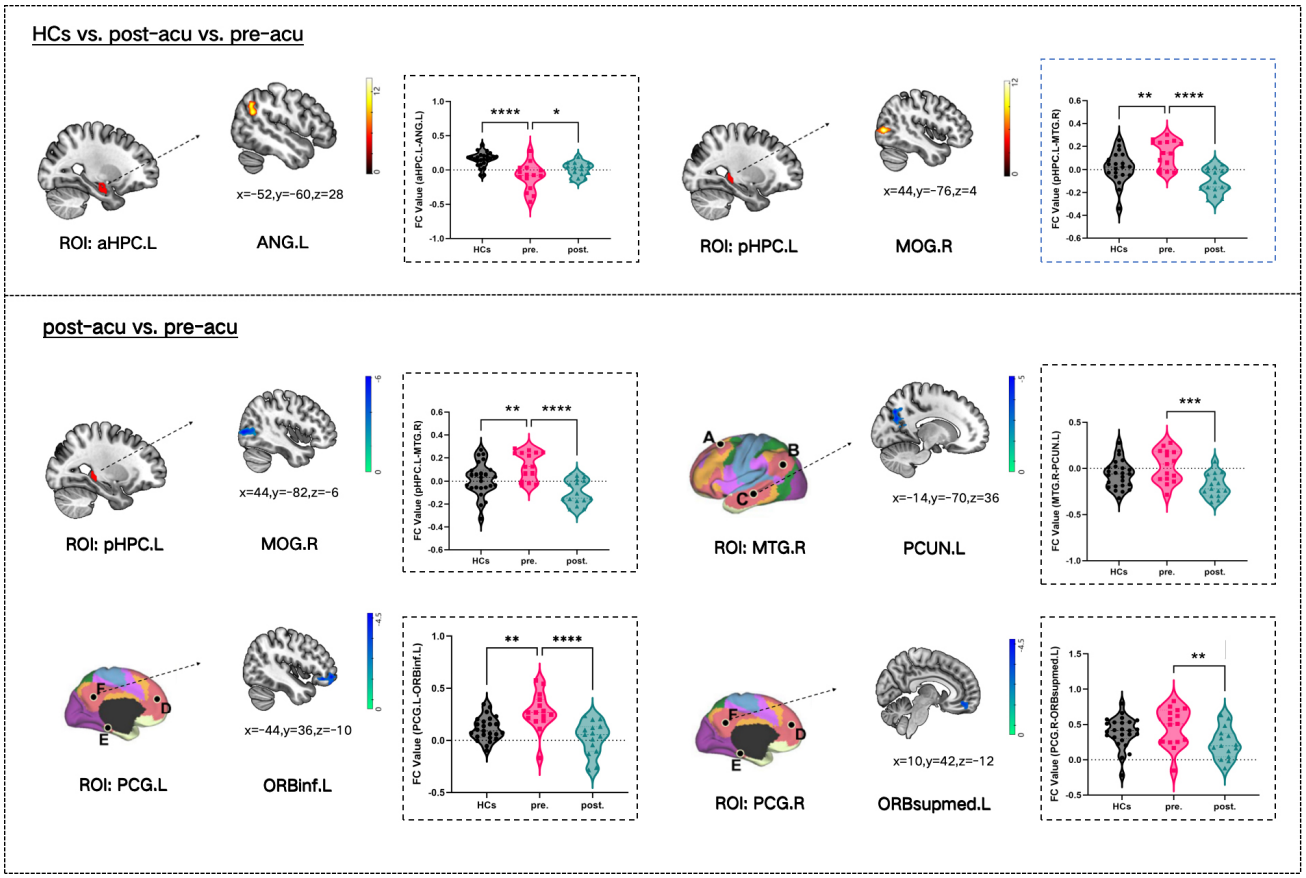

Fig. 4. Group-level and within-group resting-state functional connectivity results after AZASE. (A) Resting-state functional connectivity values in HCs, pre-acu, and post-acu groups; statistical annotations are shown only for HCs vs. pre-acu and pre-acu vs. post-acu comparisons, whereas the HCs vs. post-acu comparison is presented for descriptive visualization only. (B) Post-acu vs. pre-acu comparisons. Data are presented as violin plots with individual data points. *$p < 0.05$, **$p < 0.01$, ***$p < 0.001$, ****$p < 0.0001$.

Notably, the most aligned behavioral alterations were seen in tasks involving executive-control performance, involving Flanker interference (inhibition), Stroop interference (interference control), and N-back performance (working-memory updating). These processes are usually linked to the frontoparietal brain network (FPN) and the cingulo-opercular network-level rather than to the hippocampus or DMN by itself [35]. Nevertheless, the hippocampus and DMN do not operate in isolation; they interact dynamically with the FPN during cognitively demanding tasks, especially when mnemonic retrieval and cognitive control must be coordinated [36]. Moreover, working mnemonic, as evaluated by the N-back task, can recruit the hippocampus when information must be maintained and manipulated over short delays [37]. Thus, the hippocampal-DMN shifts identified here might reflect wider network-level reorganization that could indirectly support executive-control performance, rather than indicating that the hippocampus or DMN is the main neural substrate of executive-control control.

These longitudinal clinical findings should be viewed carefully. Given that repeated assessments were performed solely in the T2DACD group, retest associations, expectation-related associations, regression to the mean, and other non-specific influences cannot be excluded. The results therefore should not be viewed as conclusive data of a particular intervention association. Nevertheless, the consistency of shifts among several cognitive domains provides initial rationale for further testing in adequately well-controlled trials. The effect sizes identified in this pilot sample (Cohen's dz ranging from 0.66 to 2.04) may help inform sample-size calculations for subsequent conclusive studies.

4.2 Alterations in Hippocampal-Cortical Coupling

A notable observation in this exploratory investigation was that behavioral alterations were accompanied by coherent RSFC alterations including hippocampal subregions and cortical association areas. The anterior and posterior portions of the hippocampus have distinct functional profiles along the hippocampal long axis [16]. The anterior hippocampus is greater strongly connected with anterior DMN and limbic areas and is involved in affective and mnemonic encoding processes, whereas the pos-

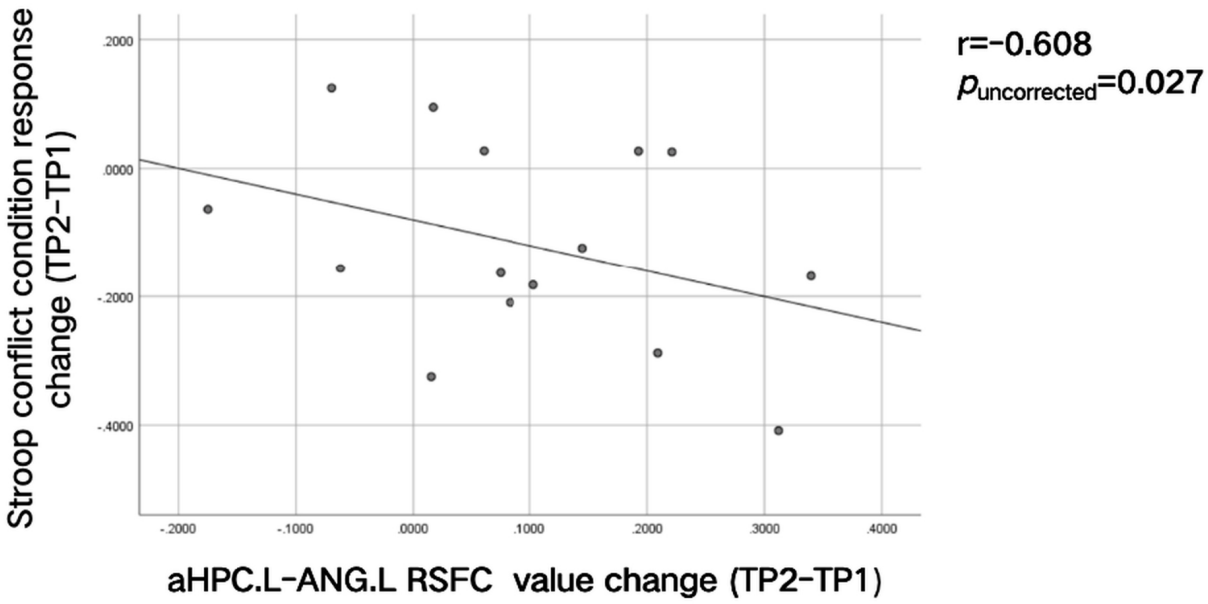

Fig. 5. Exploratory association between change in aHPC.L–ANG.L RSFC and change in Stroop-conflict reaction time after AZASE. Note: The correlation shown is uncorrected (p = 0.027) and did not remain significant after Bonferroni correction. Abbreviations: RSFC, resting-state functional connectivity.

terior hippocampus shows stronger network-level connections with posterior DMN and sensory-association cortices and supports spatial and contextual processing [16]. The hippocampus has a core role in mnemonic formation and wider cognitive integration [38], while the ANG is a heteromodal association area within the DMN that contributes to episodic retrieval, semantic integration, and memory-related cognitive function [39,40,41].

One of the most important findings involved the aHPC.L-ANG.L connection. The postintervention profile for this connection indicated a directional trend toward the HC comparison pattern. Because direct postintervention versus HC statistical contrasts were not conducted for the extracted cluster values, the present finding should not be read as conclusive normalization. It is more appropriately described as a pattern aligned with partial normalization, or with improved network-level efficiency. Importantly, given that the HC group was not followed longitudinally, the observation that TP2 values trended numerically toward the HC pattern does not establish that the alterations were specifically attributable to AZASE. Nor does it exclude the possibility that the trend reflected regression to the mean, retest associations, or natural disease fluctuation. The present cautious interpretation is consistent with data that the hippocampus-ANG mechanism contributes to memory-guided cognitive function and higher-order integrative processing [42]. The involvement of the anterior hippocampus in the present connection is also consistent with its role in affective and mnemonic encoding processes [43], which aligns with the identified changes in both cognitive and affective indices in the present work.

The exploratory inverse association between shift in aHPC.L-ANG.L coupling and shift in Stroop-conflict response time is biologically reasonable, but it did not survive adjustment for multiple contrasts. This result should therefore be viewed only as hypothesis-generating, not as data of a confirmed imaging-behavior pathway. Although the hippocampus and ANG are classically associated with episodic and semantic mnemonic [42], the aHPC.L-ANG.L mechanism might also contribute to executive-control processes when tasks require integration of memory-based information with goal-directed behavior [44]. The directional trend in the present connection, together with shifts in Stroop-conflict response time, is aligned with the possibility that hippocampal-DMN reorganization might relate to wider cognitive processes beyond mnemonic, including the executive-control demands of interference processing. This interpretation remains tentative.

We additionally noted decreased postintervention coupling between the pHPC.L and MOG.R. Given the role of the pHPC in contextual and spatial aspects of mnemonic and the role of occipital areas in visual information processing, this shift may descriptively reflect reduced reliance on inefficient or compensatory connectivity. This interpretation remains tentative and could not be confirmed with the present design. The posterior hippocampus preferentially connects with posterior cortical areas, involving occipital areas, and is more engaged in visuospatial and con-

textual processing [45]. Its involvement in this connection might thus relate to the visuospatial and attentional components of the noted cognitive observed changes in T2DACD. Nevertheless, both increased and decreased functional coupling can reflect compensatory adaptation depending on the network-level context, and the current dataset do not establish a single underlying pathway [46].

4.3 Intra-DMN Coupling Changes

Beyond hippocampal-cortical associations, postintervention decreases in coupling were observed between the MTG.R and PCUN.L and between the posterior cingulate gyrus and orbitofrontal or medial frontal areas. These areas are notable components of higher-order association networks and the DMN [47]. In the Yeo 7-network-level parcellation, the DMN contains several functionally distinct subregions: DefaultC, centered on the posterior cingulate cortex and medial prefrontal cortex, serves as a major integrative hub involved in self-referential processing and episodic mnemonic; DefaultD, centered on the angular gyrus and lateral temporal cortex, is involved in semantic and language-related processing; and DefaultF, centered on the medial temporal lobe, contributes to mnemonic encoding and retrieval [47]. The within-group connectivity changes observed here, including MTG.R (a DefaultD area) to PCUN.L (a DefaultC area) and posterior cingulate gyrus to orbitofrontal and medial frontal areas, spanned multiple DMN hubs. This pattern suggests network-level reorganization during the treatment period rather than an isolated node-specific effect. Altered DMN connectivity has been presented in T2DM and diabetes-related cognitive impairment, and the current preliminary findings are generally aligned with earlier reports of network-level dysregulation including memory-related and internally directed cognitive processes [48].

The DMN has traditionally been described as a task-negative network-level that deactivates during externally directed cognitive demands [49]. Increasing evidence, however, indicates that the DMN does not simply shut down during executive-control tasks; instead, it dynamically couples and decouples with the FPN according to task demands [50]. Altered DMN-FPN connectivity has been presented in aging, mild cognitive impairment, and metabolism-related disorders such as T2DM [48]. The decreased intra-DMN connectivity noted in this work, especially including DefaultC and DefaultD hubs, might reflect a trend toward a greater efficient network-level configuration that supports cognitive flexibility, a core component of executive performance [51].

Importantly, the observed RSFC within-group observed changes should not be overinterpreted as an unequivocal reversal of pathology. In certain network systems, both hyperconnectivity and hypoconnectivity may reflect compensatory processes, inefficient recruitment, or altered integration. The current dataset are therefore best viewed as evidence of treatment-associated brain network reorganization that might be compatible with improved neural efficiency, rather than as proof of a particular mechanism-oriented mechanism.

4.4 Clinical Implications and Subsequent Directions

The inclusion of a healthy appropriate control comparison group provided a helpful descriptive context for initial cognitive and imaging observations by offering a non-diabetic comparison pattern. This design also allowed visual contrast of T2DACD-TP2 patterns with the HC pattern. Nevertheless, given that the HCs were not followed longitudinally and no sham-acupuncture or attention-control T2DACD group was included, causal inference remains restricted. The present limitation is particularly relevant in acupuncture research, where sham procedures remain debated given that they might not be physiologically inert and can themselves evoke somatosensory or nonspecific responses [52,53].

Another important aspect of the findings is that cognitive and certain affective outcomes changed within the T2DACD group, whereas metabolism-related markers showed solely numerical changes. The present profile suggests that the noted clinical and imaging longitudinal changes are unlikely to be explained by short-term glucose lowering by itself. More carefully, the reported findings raise the possibility that AZASE might be associated with concurrent within-group longitudinal changes in cognitive function, emotional symptoms, and functional network organization, although the present cautious interpretation remains tentative and needs confirmation in well-controlled future trials. The present view is generally consistent with previous study suggesting that T2DACD reflects greater than glycemic burden by itself and is related to wider brain-network changes [54,55].

The relatively consistent changes in executive-control performance tasks, in the context of hippocampal-DMN changes, raise the possibility that acupuncture might influence large-scale brain network systems in a coordinated manner. One possible interpretation is that the intervention period affected the DMN-hippocampal system while indirectly supporting executive-control processes through dynamic interactions with the FPN [50]. The present careful interpretation is tentative and should be tested directly in well-controlled investigations that include network-level evaluations across multiple large-scale networks.

Subsequent investigations should prespecify main and secondary measures, include sham or active control conditions, and incorporate repeated assessment of comparator cohorts. Larger samples and clearly defined imaging-behavior hypotheses will be needed to determine whether the present signals are reproducible. Direct contrasts of extracted RSFC clinical behavioral measures between T2DACD-TP2 and HCs, together with clearer visualization of group means, dispersion, and uncertainty intervals,

would additionally improve interpretation of whether post-treatment patterns show any credible tendency toward normalization.

5. Limitations

The present investigation has multiple important limitations. First, and most importantly, it was performed as an open-label, non-randomized, uncontrolled exploratory pilot treatment without a sham-acupuncture or attention-control group. This design prevents causal attribution of the observed within-group changes to AZASE. Placebo associations, expectation-related associations, regression to the mean, retest associations on repeated cognitive testing, and other non-specific temporal or contextual factors could not be ruled out as alternative explanations. Thus, the findings should be read only as descriptive, hypothesis-generating observations, not as data of intervention effectiveness or pathway. This is a common challenge in acupuncture research given that sham procedures are frequently not physiologically inert and might themselves evoke somatosensory or biomarker responses [56,57]. Subsequent investigations should adopt randomized controlled designs with carefully justified sham or comparator conditions.

Second, postintervention evaluations were conducted with a per-protocol strategy rather than an intention-to-treat approach. Given that four individuals with T2DACD withdrew before investigation completion, solely completers contributed to the longitudinal evaluations. Attrition-related bias therefore could not be excluded. The results should be viewed as secondary clinical outcomes among individuals who completed the intervention, rather than as conclusive evidence of intervention effectiveness in all enrolled participants.

Third, the sample size was relatively limited (n = 15 for longitudinal evaluations), especially for the neuroimaging and correlation exploratory statistical analyses. This is common in pilot neuroimaging investigations, which are intended to estimate effect sizes and assess feasibility rather than to offer conclusive hypothesis testing [20]. Nonetheless, the small sample limits statistical power, reduces the ability to detect stable imaging-behavior associations after adjustment for multiple contrasts, and increases the risk of both false-positive and false-negative observations. To address this limitation, effect sizes and confidence intervals are emphasized alongside *p* values throughout the findings, because these metrics are more informative than statistical significance tests in limited independent samples. The identified effect sizes (Cohen's dz up to 2.04 for MoCA observed change) should be regarded as initial and applied with caution for future trial planning. Larger-scale cohorts are required to establish whether the identified trends are replicable and clinically meaningful. We also acknowledge that formal normality testing has limited power in limited larger samples; nevertheless, Shapiro-Wilk tests were supplemented with Q-Q plot inspection, and non-parametric alternatives were used where indicated, providing additional reassurance regarding the robustness of the conclusions.

Fourth, the HC group served as an initial comparison solely and did not undergo longitudinal follow-up. Although this design was helpful for identifying abnormal baseline patterns and assessing whether postintervention observations trended toward the HC comparison profile, it does not permit direct contrast of longitudinal change between cohorts. Future investigations should include repeated assessment of a matched comparator group to strengthen causal inference. Consequently, any noted trend toward the HC pattern at TP2 cannot be attributed to AZASE and should not be read as data of normalization or intervention effectiveness. In addition, residual confounding by unmeasured lifestyle-related factors, such as body mass index (BMI), smoking, and alcohol consumption, could not be ruled out.

Fifth, the work used seed-based exploratory analyses focused on hippocampal and DMN subregions given their strong relevance to mnemonic and diabetes-related cognitive dysfunction [13]. This hypothesis-driven strategy allowed us to examine particular hippocampal-DMN functional connections. Nevertheless, given that the most prominent behavioral within-group changes involved executive-control performance tasks, which are traditionally linked to the frontoparietal network [35], the present network-focused approach may have missed direct additional changes in the FPN or in other large-scale systems, such as salience or cingulo-opercular networks, that may be more explicitly involved in executive control. We acknowledge that the study was not planned to test additional changes in these other network systems. Future whole-brain approaches are required to define the full profile of acupuncture-related network modulation among multiple large-scale networks.

Sixth, the statistical cutoff applied for the fMRI statistical exploratory analysis requires care. We used a voxel-level cluster-defining cutoff of $p < 0.005$ (uncorrected) combined with cluster-level FWE adjustment ($p < 0.05$). Although this approach balances sensitivity and Type I error control in exploratory pilot investigations [31], the relatively lenient voxel-level cutoff may increase the risk of false-positive observations compared with more conservative procedures such as voxel-level FWE or false discovery rate (FDR) adjustment [32]. In addition, cluster-level inference based on random field theory can be sensitive to violations of its assumptions, especially in limited samples [32]. Thus, the neuroimaging results presented here should be viewed as initial and hypothesis-generating and require validation in larger-scale, independent cohorts with more stringent adjustment methods [58,59].

Finally, although the current findings raise the possibility that AZASE may coincide with longitudinal additional changes in cognitive function and brain connectivity, the biological pathways linking metabolism-related status,

emotional symptoms, and core network remodeling remain incompletely defined. Subsequent studies should integrate cognitive testing with multimodal imaging, metabolism-related indices, and, where feasible, mechanism-oriented biomarkers. Such work would help clarify whether observed changes reflect treatment-related neuromodulation, nonspecific clinical improvement, or broader interactions among metabolic, emotional, and neural systems.

6. Conclusion

In the present exploratory, open-label pilot study, participants with T2DACD indicated within-group additional changes in overall cognition, specific executive-control and working memory clinical measures, and several affective secondary clinical outcomes during an 8-week AZASE electroacupuncture treatment. These observed changes were accompanied by changes in RSFC including hippocampal-DMN and intra-DMN connections. Because the study was uncontrolled and the longitudinal sample was small, the observations should be viewed as initial and hypothesis-generating rather than as data of normalization, treatment efficacy, or a particular causal pathway. Even so, the findings offer a useful basis for further evaluation of electroacupuncture as a possible adjunctive treatment for T2DACD in adequately powered, carefully well-controlled future trials.

Availability of Data and Materials

The data that support the findings of this study are available from the corresponding authors upon reasonable request.

Author Contributions

LY: Writing—original draft, Conceptualization, Methodology, Investigation. ML: Visualization, Formal analysis, Data curation. YL: Resources, Investigation. JC: Resources, Investigation. ZL: Resources, Investigation. HZ: Formal analysis, Data curation. HH: Supervision, Conceptualization, Methodology, Writing—review & editing. HW: Funding acquisition, Supervision, Project administration, Conceptualization, Writing—review & editing. ZZ: Project administration, Conceptualization, Methodology, Writing – review & editing. All authors contributed to editorial changes in the manuscript. All authors read and approved the final manuscript. All authors have participated sufficiently in the work and agreed to be accountable for all aspects of the work.

Ethics Approval and Consent to Participate

This study was approved by the Medical Ethics Committee of the Third Affiliated Hospital of Changchun University of Chinese Medicine (Ethics Committee Approval Document No.: CZDSfYLL2020-001-01). All participants were informed of the study procedures before enrollment and provided written informed consent. The study was carried out in accordance with the guidelines of the Declaration of Helsinki.

Acknowledgment

We sincerely thank all members of the research team for their commitment and diligent efforts throughout the conduct of this study.

Funding

This work was supported by National Natural Science Foundation of China (Grant No. 82074548), Natural Science Foundation of Jilin Province (Free exploration of general projects) (Permit No. YDZJ202401680ZYTS).

Conflicts of Interest

The authors declare no conflicts of interest.

Declaration of AI and AI-Assisted Technologies in the Writing Process

During the preparation of this manuscript, the authors used ChatGPT solely to support language polishing, grammatical correction, and structural improvement. The authors confirm that its use was in full accordance with the applicable terms and conditions. Throughout the process, the tool was employed only under direct human oversight and did not replace the authors' own critical evaluation or professional judgment. All AI-assisted outputs were subsequently reviewed, revised, and validated by the authors to ensure accuracy and to minimize potential bias. The authors retain full responsibility for the originality, integrity, and final content of this publication.

Supplementary Material

Supplementary material associated with this article can be found, in the online version, at https://doi.org/10.31083/JIN52929.

References

[1] Genitsaridi I, Salpea P, Salim A, Sajjadi SF, Tomic D, James S, et al. 11th edition of the IDF Diabetes Atlas: global, regional, and national diabetes prevalence estimates for 2024 and projections for 2050. The Lancet. Diabetes & Endocrinology. 2026; 14: 149–156. https://doi.org/10.1016/S2213-8587(25)00299-2

[2] GBD 2021 Diabetes Collaborators. Global, regional, and national burden of diabetes from 1990 to 2021, with projections of prevalence to 2050: a systematic analysis for the Global Burden of Disease Study 2021. Lancet (London, England). 2023; 402: 203–234. https://doi.org/10.1016/S0140-6736(23)01301-6

[3] Srikanth V, Sinclair AJ, Hill-Briggs F, Moran C, Biessels GJ. Type 2 diabetes and cognitive dysfunction-towards effective management of both comorbidities. The Lancet. Diabetes & Endocrinology. 2020; 8: 535–545. https://doi.org/10.1016/S2213-8587(20)30118-2

[4] Palta P, Schneider ALC, Biessels GJ, Touradji P, Hill-Briggs F. Magnitude of cognitive dysfunction in adults with type 2 diabetes: a meta-analysis of six cognitive domains and the

most frequently reported neuropsychological tests within domains. Journal of the International Neuropsychological Society : JINS. 2014; 20: 278–291. https://doi.org/10.1017/S1355617713001483

[5] You Y, Liu Z, Chen Y, Xu Y, Qin J, Guo S, et al. The prevalence of mild cognitive impairment in type 2 diabetes mellitus patients: a systematic review and meta-analysis. Acta Diabetologica. 2021; 58: 671–685. https://doi.org/10.1007/s00592-020-01648-9

[6] Pal K, Mukadam N, Petersen I, Cooper C. Mild cognitive impairment and progression to dementia in people with diabetes, prediabetes and metabolic syndrome: a systematic review and meta-analysis. Social Psychiatry and Psychiatric Epidemiology. 2018; 53: 1149–1160. https://doi.org/10.1007/s00127-018-1581-3

[7] Geijselaers SLC, Sep SJS, Stehouwer CDA, Biessels GJ. Glucose regulation, cognition, and brain MRI in type 2 diabetes: a systematic review. The Lancet. Diabetes & Endocrinology. 2015; 3: 75–89. https://doi.org/10.1016/S2213-8587(14)70148-2

[8] Lin G, Yie SLJ, Guo S, Li X, Xu L. Clinical evidence of acupuncture for amnestic mild cognitive impairment: A systematic review and meta-analysis of randomized controlled trials. Complementary Therapies in Medicine. 2025; 88: 103114. https://doi.org/10.1016/j.ctim.2024.103114

[9] Han JZ, Yang Y, Wang YF, Feng JH, Song CN, Wu WJ, et al. Effectiveness and safety of Governor vessel acupuncture therapy for post-stroke cognitive impairment: A meta-analysis of randomized controlled trials. Ageing Research Reviews. 2024; 99: 102355. https://doi.org/10.1016/j.arr.2024.102355

[10] Zheng X, Lin W, Jiang Y, Lu K, Wei W, Huo Q, et al. Electroacupuncture ameliorates beta-amyloid pathology and cognitive impairment in Alzheimer disease via a novel mechanism involving activation of TFEB (transcription factor EB). Autophagy. 2021; 17: 3833–3847. https://doi.org/10.1080/15548627.2021.1886720

[11] Pan H, Huang H, Zhang L, Ma S, Yang H, Wang H. "Adjusting internal organs and dredging channel" electroacupuncture treatment prevents the development of diabetic peripheral neuropathy by downregulating glucose-related protein 78 (GRP78) and caspase-12 in streptozotocin-diabetic rats. Journal of Diabetes. 2019; 11: 928–937. https://doi.org/10.1111/1753-0407.12916

[12] Zhang L, Chen X, Wang H, Huang H, Li M, Yao L, et al. "Adjusting Internal Organs and Dredging Channel" Electroacupuncture Ameliorates Insulin Resistance in Type 2 Diabetes Mellitus by Regulating the Intestinal Flora and Inhibiting Inflammation. Diabetes, Metabolic Syndrome and Obesity : Targets and Therapy. 2021; 14: 2595–2607. https://doi.org/10.2147/DMSO.S306861

[13] Yao L, Li MY, Wang KC, Liu YZ, Zheng HZ, Zhong Z, et al. Abnormal resting-state functional connectivity of hippocampal subregions in type 2 diabetes mellitus-associated cognitive decline. Frontiers in Psychiatry. 2024; 15: 1360623. https://doi.org/10.3389/fpsyt.2024.1360623

[14] Lisman J, Buzsáki G, Eichenbaum H, Nadel L, Ranganath C, Redish AD. Viewpoints: how the hippocampus contributes to memory, navigation and cognition. Nature Neuroscience. 2017; 20: 1434–1447. https://doi.org/10.1038/nn.4661

[15] Smallwood J, Bernhardt BC, Leech R, Bzdok D, Jefferies E, Margulies DS. The default mode network in cognition: a topographical perspective. Nature Reviews. Neuroscience. 2021; 22: 503–513. https://doi.org/10.1038/s41583-021-00474-4

[16] Xie H, Illapani VSP, Reppert LT, You X, Krishnamurthy M, Bai Y, et al. Longitudinal hippocampal axis in large-scale cortical systems underlying development and episodic memory. Proceedings of the National Academy of Sciences of the United States of America. 2024; 121: e2403015121. https://doi.org/10.1073/pnas.2403015121

[17] Yeo BTT, Krienen FM, Sepulcre J, Sabuncu MR, Lashkari D, Hollinshead M, et al. The organization of the human cerebral cortex estimated by intrinsic functional connectivity. Journal of Neurophysiology. 2011; 106: 1125–1165. https://doi.org/10.1152/jn.00338.2011

[18] Andrews-Hanna JR, Smallwood J, Spreng RN. The default network and self-generated thought: component processes, dynamic control, and clinical relevance. Annals of the New York Academy of Sciences. 2014; 1316: 29–52. https://doi.org/10.1111/nyas.12360

[19] Eldridge SM, Chan CL, Campbell MJ, Bond CM, Hopewell S, Thabane L, et al. CONSORT 2010 statement: extension to randomised pilot and feasibility trials. Pilot and Feasibility Studies. 2016; 2: 64. https://doi.org/10.1186/s40814-016-0105-8

[20] Leon AC, Davis LL, Kraemer HC. The role and interpretation of pilot studies in clinical research. Journal of Psychiatric Research. 2011; 45: 626–629. https://doi.org/10.1016/j.jpsychires.2010.10.008

[21] Thabane L, Ma J, Chu R, Cheng J, Ismaila A, Rios LP, et al. A tutorial on pilot studies: the what, why and how. BMC Medical Research Methodology. 2010; 10: 1. https://doi.org/10.1186/1471-2288-10-1

[22] Desmond JE, Glover GH. Estimating sample size in functional MRI (fMRI) neuroimaging studies: statistical power analyses. Journal of Neuroscience Methods. 2002; 118: 115–128. https://doi.org/10.1016/s0165-0270(02)00121-8

[23] American Diabetes Association. 2. Classification and Diagnosis of Diabetes: *Standards of Medical Care in Diabetes-2020*. Diabetes Care. 2020; 43: S14–S31. https://doi.org/10.2337/dc20-S002

[24] Nasreddine ZS, Phillips NA, Bédirian V, Charbonneau S, Whitehead V, Collin I, et al. The Montreal Cognitive Assessment, MoCA: a brief screening tool for mild cognitive impairment. Journal of the American Geriatrics Society. 2005; 53: 695–699. https://doi.org/10.1111/j.1532-5415.2005.53221.x

[25] Standardization Administration of the People's Republic of China. Nomenclature and location of acupuncture points (GB/T 12346-2006). Beijing: Standards Press of China. 2006.

[26] Power JD, Barnes KA, Snyder AZ, Schlaggar BL, Petersen SE. Spurious but systematic correlations in functional connectivity MRI networks arise from subject motion. NeuroImage. 2012; 59: 2142–2154. https://doi.org/10.1016/j.neuroimage.2011.10.018

[27] Ciric R, Wolf DH, Power JD, Roalf DR, Baum GL, Ruparel K, et al. Benchmarking of participant-level confound regression strategies for the control of motion artifact in studies of functional connectivity. NeuroImage. 2017; 154: 174–187. https://doi.org/10.1016/j.neuroimage.2017.03.020

[28] Andrews-Hanna JR, Reidler JS, Sepulcre J, Poulin R, Buckner RL. Functional-anatomic fractionation of the brain's default network. Neuron. 2010; 65: 550–562. https://doi.org/10.1016/j.neuron.2010.02.005

[29] Williams S, Carson R, Tóth K. Moving beyond P values in The Journal of Physiology: A primer on the value of effect sizes and confidence intervals. The Journal of Physiology. 2023; 601: 5131–5133. https://doi.org/10.1113/JP285575

[30] Worsley KJ, Marrett S, Neelin P, Vandal AC, Friston KJ, Evans AC. A unified statistical approach for determining significant signals in images of cerebral activation. Human Brain Mapping. 1996; 4: 58–73. https://doi.org/10.1002/(SICI)1097-0193(1996)4:1%3C58::AID-HBM4%3E3.0.CO;2-O

[31] Lieberman MD, Cunningham WA. Type I and Type II error concerns in fMRI research: re-balancing the scale. Social Cognitive and Affective Neuroscience. 2009; 4: 423–428. https://doi.org/10.1093/scan/nsp052

[32] Eklund A, Nichols TE, Knutsson H. Cluster failure: Why fMRI

inferences for spatial extent have inflated false-positive rates. Proceedings of the National Academy of Sciences of the United States of America. 2016; 113: 7900–7905. https://doi.org/10.1073/pnas.1602413113

[33] Lee EC, Whitehead AL, Jacques RM, Julious SA. The statistical interpretation of pilot trials: should significance thresholds be reconsidered? BMC Medical Research Methodology. 2014; 14: 41. https://doi.org/10.1186/1471-2288-14-41

[34] Islam N, Hashem R, Gad M, Brown A, Levis B, Renoux C, et al. Accuracy of the Montreal Cognitive Assessment tool for detecting mild cognitive impairment: A systematic review and meta-analysis. Alzheimer's & Dementia : the Journal of the Alzheimer's Association. 2023; 19: 3235–3243. https://doi.org/10.1002/alz.13040

[35] Wood JL, Nee DE. Cingulo-Opercular Subnetworks Motivate Frontoparietal Subnetworks during Distinct Cognitive Control Demands. The Journal of Neuroscience : the Official Journal of the Society for Neuroscience. 2023; 43: 1225–1237. https://doi.org/10.1523/JNEUROSCI.1314-22.2022

[36] Deck BL, Kelkar A, Erickson B, Erani F, McConathey E, Sacchetti D, et al. Individual-level functional connectivity predicts cognitive control efficiency. NeuroImage. 2023; 283: 120386. https://doi.org/10.1016/j.neuroimage.2023.120386

[37] Owen AM, McMillan KM, Laird AR, Bullmore E. N-back working memory paradigm: a meta-analysis of normative functional neuroimaging studies. Human Brain Mapping. 2005; 25: 46–59. https://doi.org/10.1002/hbm.20131

[38] Pronier É, Morici JF, Girardeau G. The role of the hippocampus in the consolidation of emotional memories during sleep. Trends in Neurosciences. 2023; 46: 912–925. https://doi.org/10.1016/j.tins.2023.08.003

[39] Lee H, Keene PA, Sweigart SC, Hutchinson JB, Kuhl BA. Adding Meaning to Memories: How Parietal Cortex Combines Semantic Content with Episodic Experience. The Journal of Neuroscience : the Official Journal of the Society for Neuroscience. 2023; 43: 6525–6537. https://doi.org/10.1523/JNEUROSCI.1919-22.2023

[40] Bellana B, Ladyka-Wojcik N, Lahan S, Moscovitch M, Grady CL. Recollection and prior knowledge recruit the left angular gyrus during recognition. Brain Structure & Function. 2023; 228: 197–217. https://doi.org/10.1007/s00429-022-02597-5

[41] Bonner MF, Peelle JE, Cook PA, Grossman M. Heteromodal conceptual processing in the angular gyrus. NeuroImage. 2013; 71: 175–186. https://doi.org/10.1016/j.neuroimage.2013.01.006

[42] Huang S, Howard CM, Hovhannisyan M, Ritchey M, Cabeza R, Davis SW. Hippocampal Functions Modulate Transfer-Appropriate Cortical Representations Supporting Subsequent Memory. The Journal of Neuroscience : the Official Journal of the Society for Neuroscience. 2024; 44: e1135232023. https://doi.org/10.1523/JNEUROSCI.1135-23.2023

[43] Fetterhoff D, Costa M, Hellerstedt R, Johannessen R, Imbach L, Sarnthein J, et al. Neuronal population representation of human emotional memory. Cell Reports. 2024; 43: 114071. https://doi.org/10.1016/j.celrep.2024.114071

[44] Thams F, Li SC, Flöel A, Antonenko D. Functional Connectivity and Microstructural Network Correlates of Interindividual Variability in Distinct Executive Functions of Healthy Older Adults. Neuroscience. 2023; 526: 61–73. https://doi.org/10.1016/j.neuroscience.2023.06.005

[45] Snytte J, Fenerci C, Rajagopal S, Beaudoin C, Hooper K, Sheldon S, et al. Volume of the posterior hippocampus mediates age-related differences in spatial context memory and is correlated with increased activity in lateral frontal, parietal and occipital regions in healthy aging. NeuroImage. 2022; 254: 119164. https://doi.org/10.1016/j.neuroimage.2022.119164

[46] Varela-López B, Zurrón M, Lindín M, Díaz F, Galdo-Alvarez S. Compensation versus deterioration across functional networks in amnestic mild cognitive impairment subtypes. GeroScience. 2025; 47: 1805–1822. https://doi.org/10.1007/s11357-024-01369-9

[47] Shao X, Krieger-Redwood K, Zhang M, Hoffman P, Lanzoni L, Leech R, et al. Distinctive and Complementary Roles of Default Mode Network Subsystems in Semantic Cognition. The Journal of Neuroscience : the Official Journal of the Society for Neuroscience. 2024; 44: e1907232024. https://doi.org/10.1523/JNEUROSCI.1907-23.2024

[48] Ni W, Liu WV, Li M, Wei S, Xu X, Huang S, et al. Altered brain functional network connectivity and topology in type 2 diabetes mellitus. Frontiers in Neuroscience. 2025; 19: 1472010. https://doi.org/10.3389/fnins.2025.1472010

[49] Leonards CA, Harrison BJ, Jamieson AJ, Steward T, Lux S, Philipsen A, et al. A distinct intra-individual suppression subnetwork in the brain's default mode network across cognitive tasks. Cerebral Cortex (New York, N.Y. : 1991). 2023; 33: 4553–4561. https://doi.org/10.1093/cercor/bhac361

[50] Jung S, Kim JY, Jo S, Han SW. The Involvement of the Multiple Demand and Default Mode Networks in a Trial-by-Trial Cognitive Control. Brain Sciences. 2023; 13: 1247. https://doi.org/10.3390/brainsci13091247

[51] Thomas SA, Ryan SK, Gilman J. Resting state network connectivity is associated with cognitive flexibility performance in youth in the Adolescent Brain Cognitive Development Study. Neuropsychologia. 2023; 191: 108708. https://doi.org/10.1016/j.neuropsychologia.2023.108708

[52] Luo XC, Liu JL, Yao MH, Chen YM, Fan AY, Liang FR, et al. Specific effect of inserted sham acupuncture and its impact on the estimation of acupuncture treatment effect in randomized controlled trials: A systematic survey. Journal of Integrative Medicine. 2025; 23: 630–640. https://doi.org/10.1016/j.joim.2025.07.011

[53] Dincer F, Linde K. Sham interventions in randomized clinical trials of acupuncture–a review. Complementary Therapies in Medicine. 2003; 11: 235–242. https://doi.org/10.1016/s0965-2299(03)00124-9

[54] Zhang W, Fu L, Bi Y, Liu J, Li X, Zhang X, et al. Large-scale functional network connectivity mediates the associations between lipids metabolism and cognition in type 2 diabetes. Journal of Cerebral Blood Flow and Metabolism : Official Journal of the International Society of Cerebral Blood Flow and Metabolism. 2024; 44: 384–396. https://doi.org/10.1177/0271678X231204426

[55] Tahamata VM, Fan YT, Wei L, Lin YN, Martinez RM, Goh KK, et al. Domain-Specific and Domain-General Functional Brain Alterations in Type 2 Diabetes Mellitus: A Task-Based and Functional Connectivity Meta-Analysis. Brain and Behavior. 2025; 15: e70438. https://doi.org/10.1002/brb3.70438

[56] Kim TH, Lee MS, Lee H. Sham Acupuncture Is Not Just a Placebo. Journal of Acupuncture and Meridian Studies. 2022; 15: 333–335. https://doi.org/10.51507/j.jams.2022.15.6.333

[57] Kim TH, Lee MS, Birch S, Alraek T. Plausible Mechanism of Sham Acupuncture Based on Biomarkers: A Systematic Review of Randomized Controlled Trials. Frontiers in Neuroscience. 2022; 16: 834112. https://doi.org/10.3389/fnins.2022.834112

[58] Woo CW, Krishnan A, Wager TD. Cluster-extent based thresholding in fMRI analyses: pitfalls and recommendations. NeuroImage. 2014; 91: 412–419. https://doi.org/10.1016/j.neuroimage.2013.12.058

[59] Costa T, Liloia D, Cauda F, Fox PT, Mutta FD, Duca S, et al. A Minimum Bayes Factor Based Threshold for Activation Likelihood Estimation. Neuroinformatics. 2023; 21: 365–374. https://doi.org/10.1007/s12021-023-09626-6